



Since January 2020 Elsevier has created a COVID-19 resource centre with free information in English and Mandarin on the novel coronavirus COVID-19. The COVID-19 resource centre is hosted on Elsevier Connect, the company's public news and information website.

Elsevier hereby grants permission to make all its COVID-19-related research that is available on the COVID-19 resource centre - including this research content - immediately available in PubMed Central and other publicly funded repositories, such as the WHO COVID database with rights for unrestricted research re-use and analyses in any form or by any means with acknowledgement of the original source. These permissions are granted for free by Elsevier for as long as the COVID-19 resource centre remains active.



Quantitative circular flow immunoassays with trained object recognition to detect antibodies to SARS-CoV-2 membrane glycoprotein

Ryan Yuki Huang^a, Deron Raymond Herr^{b,*}

^a Canyon Crest Academy, San Diego, USA

^b Department of Biology, State University, San Diego, USA



ARTICLE INFO

Article history:

Received 27 April 2021

Accepted 19 May 2021

Available online 29 May 2021

Keywords:

Circular flow immunoassay

COVID-19

Membrane glycoprotein

SARS-CoV-2

YOLO v4

ABSTRACT

Amidst infectious disease outbreaks, a practical tool that can quantitatively monitor individuals' antibodies to pathogens is vital for disease control. The currently used serological lateral flow immunoassays (LFIAs) can only detect the presence of antibodies for a single antigen. Here, we fabricated a multiplexed circular flow immunoassay (CFIA) test strip with YOLO v4-based object recognition that can quickly quantify and differentiate antibodies that bind membrane glycoprotein of severe acute respiratory syndrome coronavirus 2 (SARS-CoV-2) or hemagglutinin of influenza A (H1N1) virus in the sera of immunized mice in one assay using one sample. Spot intensities were found to be indicative of antibody titers to membrane glycoprotein of SARS-CoV-2 and were, thus, quantified relative to spots from immunoglobulin G (IgG) reaction in a CFIA to account for image heterogeneity. Quantitative intensities can be displayed in real time alongside an image of CFIA that was captured by a built-in camera. We demonstrate for the first time that CFIA is a specific, multi-target, and quantitative tool that holds potential for digital and simultaneous monitoring of antibodies recognizing various pathogens including SARS-CoV-2.

© 2021 The Authors. Published by Elsevier Inc. This is an open access article under the CC BY license (<http://creativecommons.org/licenses/by/4.0/>).

1. Introduction

The global outbreak of severe acute respiratory syndrome coronavirus 2 (SARS-CoV-2), causing coronavirus disease 2019 (COVID-19), has had pronounced global impacts, affecting international travel, social interactions and world economy. Real time reverse transcription-polymerase chain reaction (RT-PCR), one of the fastest and most accurate methods of amplifying viral ribonucleic acid (RNA), has been used to identify and track the SARS-CoV-2 virus [1]. However, detection of antibodies induced by natural infection and vaccination may be needed for suspected false-negative RT-PCR results [2], identification of previous, resolved infection, and calculation of protective immunity. At present, first-generation mRNA vaccines against COVID-19 by Pfizer and Moderna companies are approved the United States Food and Drug Administration (FDA) as a possible means of providing herd

immunity providing herd immunity [3]. Although promising, these first-generation COVID-19 vaccines may not be the ultimate panacea for people to travel during the pandemic, as the heterogeneity in vaccine response have yet to be investigated. As such, a mediatory solution that can track those who have antibody-elicited protective immunity by measuring individual antibody titers would be an invaluable tool for disease control in present and future outbreaks.

Currently, personal Immunization Cards used in the United States of America (USA) are the only antibody tracking method, wherein previous vaccinations are listed since the injection of the first vaccine. However, antibody titers are not quantitative, and individual antibody fluctuations following vaccinations are not considered. It has been documented that antibodies remain stable for only five months in mild-to-moderate COVID-19 patients [4], indicating that antibody-based immunity may fade in as little as few months after infection. Furthermore, the stability and duration of antibody titers for COVID-19 vaccines have not yet been determined. SARS-CoV-2 expresses nonstructural replicase polyproteins and structural proteins, namely spike, envelope, membrane glycoprotein, and nucleocapsid [5]. While the spike protein has been

* Corresponding author.

E-mail addresses: rhuang53@gmail.com (R.Y. Huang), dherr@sdsu.edu (D.R. Herr).

used as the leading target antigen in vaccine development, viral mutations on spike protein, such as the N501Y strain with a N501Y amino acid substitution in the receptor-binding domain (RBD) of the spike protein, may diminish the efficacy of first-generation vaccines targeting spike protein [6]. In contrast, other SARS-CoV-2 proteins may be relatively conserved [7] and have been selected for diagnostic kits for COVID-19 [8].

Assays, such as Immuno-COV (jointly developed by Vyriad and Regeneron Inc.) and NeuCOVIX (Axim Biotechnologies, Inc.), have developed serologic tests for detection of the neutralizing antibodies to the SARS-CoV-2 spike protein. However, both Immuno-COV and NeuCOVIX tests are cell-based *in vitro* assays, which require trained laboratorians and specialized instruments. Designing Immunity Passports, companies, including Sienna (T&D Diagnostics Canada) and Cellex (North Carolina, USA), are developing serological lateral flow immunoassays (LFIAs) to detect human anti-SARS-CoV-2 immunoglobulin G/M (IgM/IgG) by binarily identifying those with antibodies as seropositive, while those without as seronegative [9,10]. However, the application of LFIAs as Immunity Passports faces many problems including 1) antibody titers are not usually quantified nor digitally transformed to portable devices like smartphones for travelers; and 2) “linearly-shaped LFIAs are not able to detect multiple antibody titers in one reaction nor differentiate distinct antibodies such as SARS-CoV-2 from influenza viruses.

The advantage of LFIAs lies in quick detection by reducing turn-around time to receive results. However, most reactions in LFIAs for antibody detection only allow for the analysis of antibodies toward a single antigen. Moreover, the use of separate LFIA reactions to compare different antibodies may increase the inaccuracy of results due to variations in sample amounts and reaction time. Although integration of LFIA and antibody microarrays [11] can achieve multi-antigen detection in one assay, quantifying this type of LFIA is similar to fluorescence LFIA [12] which requires data readers comprised of image analysis computer software and specialized equipment to detect signals on the test strips. Here, a circular flow immunoassay (CFIA), or “All-In-One” assay, was fabricated by optimizing the components from the LFIAs into a circular array, allowing to simultaneously capture circulating antibodies from blood samples, synchronously detecting multiple antibodies using just a few microliters of sample. Most importantly, quantitative CFIAs can be displayed in real time by a camera without expressive equipment and highly trained professional personnel.

2. Materials and methods

2.1. Recombinant proteins and sera

A plasmid carrying a gene encoding membrane glycoprotein (YP_009724393.1) of SARS-CoV-2 (Genebank accession: NC_045512.2) or hemagglutinin (Accession number: ACP41105) of swine origin influenza A (H1N1) virus (S-OIV) San Diego/01/09 (SD/H1N1-S-OIV) was transformed into *Escherichia coli* (*E. coli*) BL21 (DE3) competent cells (Invitrogen, Carlsbad, CA, USA). Proteins were purified using a ProBond Purification System (Invitrogen). Spike protein (YP_009724390.1) (approximately 600 kDa) of SARS-CoV-2 was expressed in human embryonic kidney (HEK) 293 cells and contained the whole extracellular domains of S1 (with RBD) and S2 from residue 14 to 1209 [13]. Methods for determination of antibody titer were described in Supplementary material.

2.2. Antibody detection using LFIA

A LFIA, which consisted of three pads (sample, conjugate, and absorbent pads), and one nitrocellulose (NC) membrane

(Membrane Technologies Inc., Harrisburg, PA, USA), with test and control zones was created. For preparation of staphylococcal protein A (SPA)-conjugated gold nanoparticles (AuNPs), 1 mM HAuCl₄ (Sigma, St. Louis, MO, USA) in double-distilled water was boiled at 200 °C. The trisodium citrate dihydrate (1%) was added to the boiling solution before gradually cooling down at the room temperature. Protein A of *Staphylococcus aureus* (20 µg) (Sigma) was mixed with the AuNPs in 1 mL borax buffer containing boric acid and sodium borax, pH 5–6 for conjugation. After 30 min of incubation at room temperature, 1% bovine serum albumin (BSA) in phosphate buffered saline (PBS) was pipetted into the conjugate solution for blocking for 30 min. After centrifugation at 12,000×g for 20 min, the supernatant was removed and the pellet with SPA-conjugated AuNPs was resuspended in 3 mL of conjugate washing buffer (1% BSA in 2 mM borax, pH 9.0) before measurement of optical density (OD) by spectrophotometer at 525 nm absorbance. The SPA-conjugated AuNPs (100 µL) was dropped onto the conjugate pad. Proteins and rabbit anti-mouse IgG (H + L) (ThermoFisher Scientific, Waltham, MA USA) were pipetted onto NC membranes. The mouse sera (200 µL) were added onto the sample pad to start reaction.

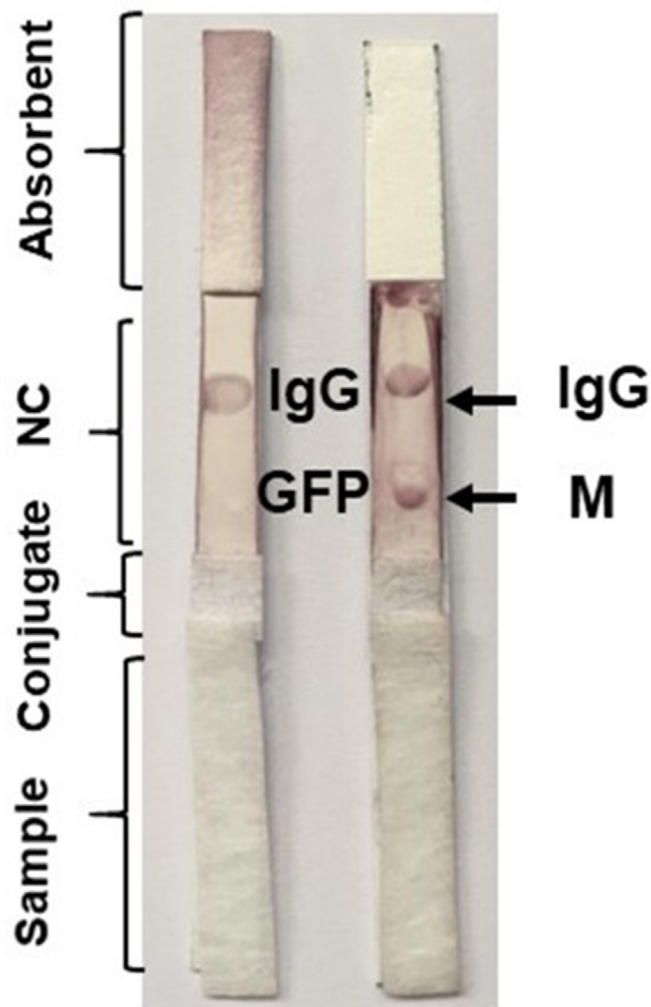


Fig. 1. Detection of antibodies to SARS-CoV-2 membrane glycoprotein by LFIA. Linear LFIA are shown, where recombinant GFP, a control protein, or SARS-CoV-2 membrane glycoprotein (M) (3 µg) were spotted on the test line of an NC membrane. The anti-mouse IgG (H + L) (3 µg) was spotted on the control line of the NC membrane.

2.3. Fabrication of CFIA

The CFIA, namely an “All-In-One” assay, was composed of a circle-shaped conjugate, a ring-shaped NC membrane, and a square absorbent pad with an open circle in the center. The conjugate pad and NC membrane were stacked from top to bottom. The absorbent pad was glued around the border of a NC membrane. The conjugate pad and NC membrane partially overlapped to allow antibodies captured SPA-conjugated AuNPs flow through to interact with proteins or anti-mouse IgG (H + L) on NC membrane.

2.4. Spots as objects for detection

For detecting spots formed by interaction of proteins with antibodies captured SPA-conjugated AuNPs, YOLO v4, a one stage detector with the ability to make rapid, real-time predictions [14], was used. The YOLO v4 network architecture was comprised of four parts: input, backbone, neck, and dense prediction. During execution, the object detector received an image as an input, and the essential features were extracted by a Cross Partial Network (CSPNet) strategy through a convolutional neural network backbone called CSPDarknet53. Consequently, in the neck layer, YOLO v4 employed a modified Path Aggregation Network (PAN), a modified Spatial Attention Module (SAM), and Spatial Pyramid Pooling (SPP) to add extra layers. The final dense prediction layer predicted both class probabilities and bounding box coordinates by dividing the image into a $S \times S$ grid, wherein each grid cell predicted bounding boxes and confidence scores. Bounding box coordinates (x, y, w, h) were parameterized and confidence scores were derived from the product of the probability of an object and its intersection over union (IOU). To distinguish different class of objects, the conditional class probabilities were calculated [15,16]. The architecture of YOLO v4 was based on mathematical operations. Dense prediction used a linear activation function while other layers used the leaky rectified linear activation [15,17]. Method for training the detection software for spot quantification was described in Supplementary material.

2.5. Statistical analysis

The unpaired *t*-test for data analysis was conducted using GraphPad Prism software (GraphPad Software, San Diego, CA, USA). The statistical significance was determined by *P*-values as follows: *P*-values of <0.05 (*), <0.01 (**), and <0.001 (***). The mean \pm standard deviation (SD) was obtained from at least three separate experiments.

3. Results

3.1. Detection of antibodies to SARS-CoV-2 membrane glycoprotein in mouse sera using LFIA

A linear LFIA (Fig. 1), consisting of three pads (sample, conjugate, and absorbent pads) and one NC membrane, was constructed using SPA-conjugated AuNPs to detect the antibodies to the target protein. The target protein and rabbit anti-mouse IgG (H + L) were spotted on the surface of an NC membrane as the test and control zones, respectively. Fc regions of antibodies in the sera were captured by SPA coated on the surface of AuNPs. Antibodies captured by SPA-conjugated AuNPs bound to the protein in the test zone, while the rest interacted with anti-mouse IgG (H + L). A positive result was confirmed visually by the presence of an intense purple spot that developed on the LFIA within 15 min. After adding 5% sera of mice immunized with SARS-CoV-2 membrane glycoprotein onto sample pads, the purple spots derived from interaction of antibodies with SPA-conjugated AuNPs appeared on NC membranes spotted with $3 \mu\text{g}$ SARS-CoV-2 membrane glycoprotein, but not control green fluorescent protein (GFP) (Fig. 1), demonstrating the feasibility of using LFIA to detect the specific antibodies to SARS-CoV-2 membrane glycoprotein in sera of immunized mice.

Subsequently, a Two-In-One LFIA was fabricated by connecting the ends of two LFIA (Fig. 2), where the membrane glycoprotein of SARS-CoV-2 or hemagglutinin of SD/H1N1-S-OIV [18] was spotted on NC membranes, establishing that bidirectional flow can allow for the synchronic detection of two antibodies in one sample. Sera from mice immunized with GFP, SARS-CoV-2 membrane

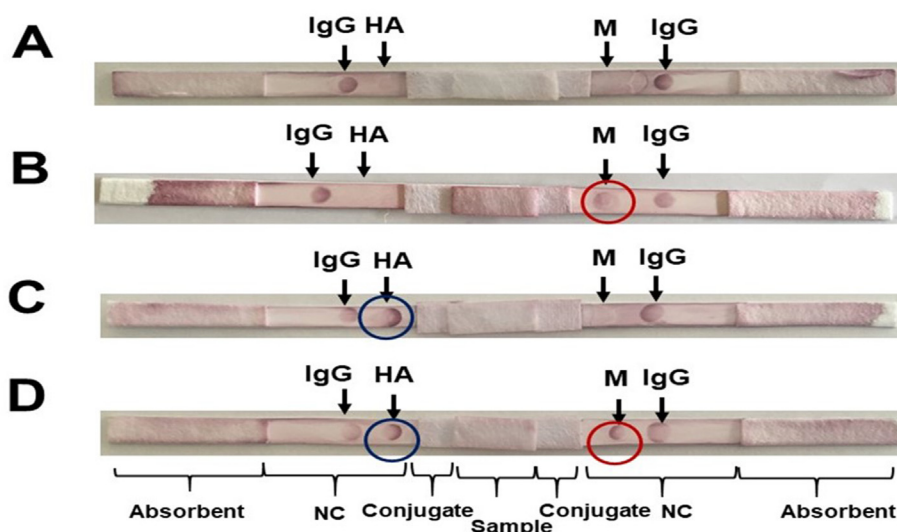


Fig. 2. Differentiation of antibodies to SARS-CoV-2 membrane protein from antibodies to SD/H1N1-S-OIV hemagglutinin. The “Two-In-One” LFIA was fabricated by connecting two LFIA with a shared sample pad. Recombinant membrane glycoprotein (M) of SARS-CoV-2 or hemagglutinin (HA) of SD/H1N1-S-OIV ($3 \mu\text{g}$) were spotted on each LFIA. The anti-mouse IgG (H + L) ($3 \mu\text{g}$) was spotted on the control line of the NC membrane. 5% sera ($200 \mu\text{L}$) from ICR mice immunized with GFP (A), membrane glycoprotein (B), or hemagglutinin (C) were inserted into the sample pad. (D) Sera from mice immunized with membrane glycoprotein or hemagglutinin were mixed in a 1:1 (v/v) ratio before inserting into the sample pad. Antibodies to membrane glycoprotein (red circles) or hemagglutinin (blue circles) were differentiated. (For interpretation of the references to color in this figure legend, the reader is referred to the Web version of this article.)

glycoprotein or SD/H1N1-S-OIV hemagglutinin were added onto the sample pads of Two-In-One LFIA. Sera from mice immunized with GFP did not react to the membrane glycoprotein or hemagglutinin antigen. Purple spots on Two-In-One LFIA indicated that antibodies to SARS-CoV-2 membrane glycoprotein in sera of immunized mice can bind the SARS-CoV-2 membrane glycoprotein, not SD/H1N1-S-OIV hemagglutinin. Antibodies to SD/H1N1-S-OIV hemagglutinin exclusively bind the hemagglutinin antigen. Purple spots derived from the reaction of antibodies to membrane glycoprotein and hemagglutinin were concurrently detected only when mixed sera from mice immunized with membrane glycoprotein or hemagglutinin were added onto a sample pad. The result indicated that there was no antigenic cross-reactivity between antibodies to membrane glycoprotein and hemagglutinin.

3.2. CFIA for simultaneous detection of antibodies, object detection and background subtraction

The CFIA, also named as All-In-One assay, was assembled for detecting multiple antibodies by allowing multidirectional, radial flow using just one sample. Multiple positions on an NC membrane were created for spotting numerous proteins which can be recognized by their specific antibodies in sera. Commonly, color intensity quantifications rely on imaging software, such as National Institutes of Health (NIH) ImageJ, which requires the user to draw and denote area region of interest to quantify intensities in an image [19]. As a result, quantifications cannot be instantaneously determined and are often subjective to human error due to the ambiguity of the spot areas. The use of deep learning to help create well-defined spot areas is a solution for an accurate quantification [20]. Here, identifications of spot areas on CFIA were performed by YOLO v4 object detection software [14]. YOLO v4 divided the image into a $S \times S$ grid and predicted bounding boxes, individual confidence score, and class probabilities for each grid cell. With high confidence scores in a defined class, an object, or target area in a bounding box, the target spot can be identified and extracted for color intensity measurement.

To illustrate the process, one representative CFIA was shown, spotted with membrane glycoprotein, spike protein of SARS-CoV-2, SD/H1N1-S-OIV hemagglutinin and anti-mouse IgG (H + L) (Fig. 3A). Sera (5% sera with a titer at 1:51,200 in PBS) of mice immunized with SARS-CoV-2 membrane glycoprotein were added onto a sample pad. When analyzing the image using only ImageJ, the purple residues remained, resulting in process pollution of the color intensities. However, when paired with YOLO v4 deep learning, the two spots derived from interaction of antibodies with membrane glycoprotein and anti-mouse IgG (H + L), respectively, were clearly identified, and the background residues were subtracted from analysis (Fig. 3B and C).

3.3. Concurrent detection of different antibodies in CFIA

Since CFIA allows the immobilization of multiple proteins, it can fully differentiate the detected antibodies from others. The membrane glycoprotein of SARS-CoV-2, hemagglutinin of SD/H1N1-S-OIV, and anti-mouse IgG (H + L) were spotted on an NC membrane of a CFIA. Sera with different antibodies were created by mixing sera from Institute of Cancer Research (ICR) mice immunized with membrane glycoprotein of SARS-CoV-2 and hemagglutinin of SD/H1N1-S-OIV in a 1:1 ratio. After application of mixed sera (200 μ L) onto a SPA-conjugated AuNPs pre-loaded conjugate pad, three purple spots appeared concurrently on a NC membrane of a CFIA (Fig. 3D). The intensities of purple spots derived from the interaction of antibodies to membrane glycoprotein and hemagglutinin, respectively, were quantified relative to those of antibodies

captured by anti-mouse IgG (H + L) (Fig. 3E). The result demonstrated the capability of CFIA to distinguish different antibodies in sera through a single assay.

4. Discussion

Several mutations in SARS-CoV-2 spike protein and nucleocapsid protein have been reported across the globe [21]. In contrast, the membrane glycoprotein is conserved across the β -coronaviruses. According to the prediction of the transmembrane helix topology in a three-dimensional (3-D) model [22], the N- and C-terminal portions of the membrane glycoprotein were exposed outside and inside the particle of SARS-CoV-2, respectively. Both B-cell and T-cell epitopes within a highly conserved region of membrane protein have been revealed [23,24]. Results from a recent study demonstrated that membrane glycoprotein inhibited the type I and III interferon production by targeting the signaling mediated by retinoic acid-inducible gene I (RIG-I) and melanoma differentiation-associated gene 5 (MDA-5) [25]. The phosphorylated interferon regulatory factor 3 (IRF3), a transcription factor, can be translocated to the nucleus, leading to the induction of genes encoding interferon and other proinflammatory cytokines [26]. The SARS-CoV-2 membrane glycoprotein can interact with RIG-I, mitochondrial antiviral signaling (MAVS), and TANK-binding kinase 1 (TBK1), impeding the phosphorylation, nuclear translocation, and activation of IRF3. Since membrane glycoprotein is relatively conserved and has fewer mutations, the protein is selected for detection of its antibodies on CFIA. Neutralizing antibodies play a chief role in protective immunity [27]. The whole recombinant membrane glycoprotein, which includes non-neutralizing domains was spotted on either LFIA (Fig. 1) or CFIA (Fig. 3). Although results in Fig. 1 indicated that recombinant membrane glycoprotein can bind to antibodies in sera of mice immunized with membrane glycoprotein, not GFP, future work will include determining which epitopes in the membrane glycoprotein can generate neutralizing antibodies that can block the formation of a multi-protein complex formed by the interaction of membrane glycoprotein with RIG-1, MAVS, and TBK-1. Spotting a fragment of membrane glycoprotein containing neutralizing epitopes, rather than a whole protein, will allow CFIA to detect the levels of neutralizing antibodies in samples.

The FDA recommendations in support of a pre Emergency Use Authorization (EUA)/EUA for SARS-CoV-2 antibody tests have been announced [28]. For approval, validation studies, including cross-reactivity, class specificity, linearity, and limit of quantitation (LoQ) for SARS-CoV-2 antibody tests, are required. In our study, recombinant membrane glycoprotein of SARS-CoV-2 and hemagglutinin of influenza A virus H1N1 were spotted on a Two-In-One LFIA (Fig. 2). Results from this Two-In-One LFIA assay identified antibodies generated by mice immunized with membrane glycoprotein that did not cross-react to the hemagglutinin of SD/H1N1-S-OIV. However, since the amino acid sequence of membrane glycoprotein of SARS-CoV-2 shares high identity to other strains of the β -coronaviruses, false positive results [29] may appear on CFIA due to previous exposure to closely-related β -coronaviruses. Spotting membrane glycoproteins from various β -coronaviruses on a CFIA may improve the viral specificity of detecting antibodies to SARS-CoV-2. Currently, most COVID-19 vaccines target SARS-CoV-2 spike protein. However, when CFIA was immobilized both membrane glycoprotein and spike protein, it will be able to distinguish between immunization and previous exposure to SRAS-CoV-2.

Protein A, which can bind Fc regions of immunoglobulins, was used to prepare SPA-conjugated AuNPs for localization and capture of various antibodies from sera. It has been documented that protein A exerts distinct affinity to various classes of immunoglobulins

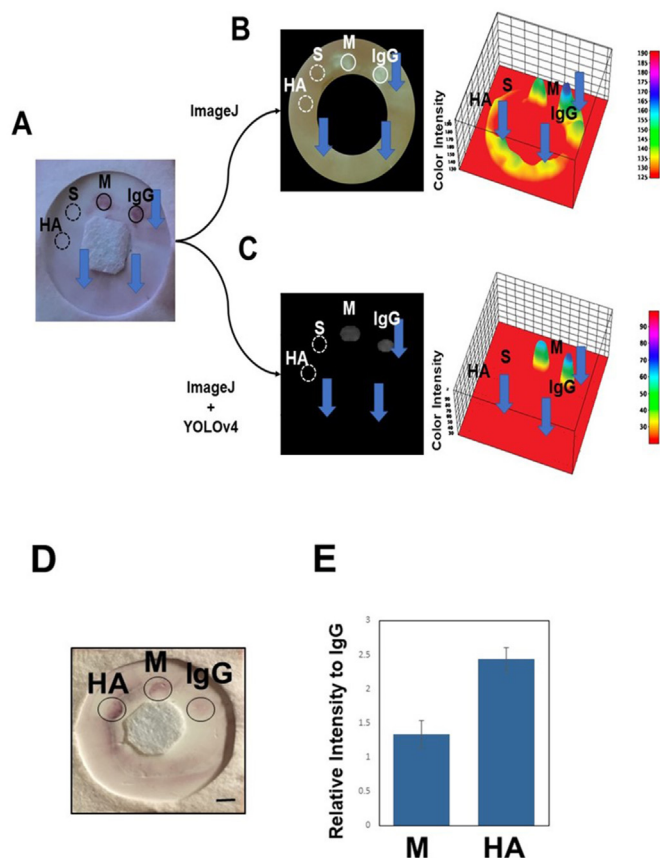


Fig. 3. Spot quantification and simultaneous detection of SARS-CoV-2 membrane glycoprotein and SD/H1N1-S-OIV hemagglutinin on a CFIA. (A) A CFIA was spotted with 3 μg of SARS-CoV-2 membrane glycoprotein (M) (Spot [1]), anti-mouse IgG (H + L) (Spot [2]), SARS-CoV-2 spike protein (S) and SD/H1N1-S-OIV hemagglutinin (HA). Purple background residues were found and denoted with blue arrows shown above. (B) Using only ImageJ, the input CFIA was converted into grayscale with purple background remaining. A 3-D surface plot was generated, highlighting the color intensities of unnecessary components with blue arrows. (C) With the same CFIA input, ImageJ was used in conjunction with YOLO v4. Once the image was converted to grayscale and spots ([1,2]) were detected, all unnecessary background components were subtracted. The subtraction was confirmed using a 3-D surface plot, which displayed no presence of purple residue. (D) A CFIA was spotted with three proteins which were 3 μg of SARS-CoV-2 membrane glycoprotein (M), SD/H1N1-S-OIV hemagglutinin (HA) and anti-mouse IgG (H + L). Sera (200 μL) from mice immunized with membrane glycoprotein or hemagglutinin were mixed in a 1:1 (v/v) ratio and dropped onto a conjugate pad. The appearance of purple spots indicated the binding of antibodies in the mixed sera to their specific proteins. (E) Relative intensities of purple spots of membrane glycoprotein (M/IgG) or hemagglutinin (HA/IgG) to those of anti-mouse IgG (H + L) were quantified by ImageJ with YOLO v4. A representative image was shown. Results as mean \pm SD were obtained from three independent experiments. (For interpretation of the references to color in this figure legend, the reader is referred to the Web version of this article.)

(IgG, IgM and IgA) in different species [30]. Protein A from *Staphylococcus aureus* has a higher affinity for human IgG (IgG1 and IgG2) than IgM and IgA. Although antibodies to membrane glycoprotein quantified by CFIA in this study may be predominately IgG, detection of IgG and/or IgA that is normally generated during the early phase of infection [31] could be achieved by replacing protein A with protein L [32], a *Peptostreptococcus magnus* protein that binds to representatives of most antibody classes. Although mixed sera from immunized mice were used (Figs. 2 and 3D, E), future work includes examining the feasibility of CFIA to differentiate various antibodies in COVID-19 patients.

The multiplex format of CFIA make it possible to simultaneously detect multiple antibodies from blood samples in one

assay. Spotting IgG (H + L) as a control was conducted to normalize the reaction of detected proteins. Normalization of readings of the spot intensities by IgG (H + L) can minimize the variation due to differing amounts of blood samples loaded onto conjugate pads by different individuals when CFIA are used in the field. In summary, unlike LFIA, CFIA were constructed to allow for concurrent measurements of multiple antibodies in a single reaction using only one sample. Antibodies in sera of immunized mice that bound to the membrane glycoprotein of SARS-CoV-2 exhibit an intense purple spot that was normalized with spotting of anti-mouse IgG (H + L). Intensities of purple spots corresponding to antibody titers on CFIA were quantified by pre-trained YOLO v4 in conjunction with ImageJ. Antibodies to membrane glycoprotein of SARS-CoV-2 can be differentiated from those to hemagglutinin of SD/H1N1-S-OIV, revealing the capability of CFIA to distinguish different antibodies in sera through a single assay. CFIA can be performed for on-site detection of antibodies to SARS-CoV-2 membrane glycoprotein and differentiation of other antibodies.

Author contributions

R.Y.H. and D.R.H. conceived the research and designed the experiments. R.Y.H. performed the experiments and analysed the data. R.Y.H. wrote the manuscript. D.R.H. reviewed and edited the manuscript.

Declaration of competing interest

The authors declare no conflicts of interest.

Acknowledgments

We thank Dr. Liangfang Zhang at University of California, San Diego for assistance at AuNP protein coating.

Appendix A. Supplementary data

Supplementary data to this article can be found online at <https://doi.org/10.1016/j.bbrc.2021.05.073>.

References

- [1] B.G. Andryukov, I.N. Lyapun, COVID-19 diagnostic laboratory strategies: modern technologies and development trends (review of literature), *Klin. Lab. Diagn.* 65 (2020) 757–766. <https://doi.org/10.18821/0869-2084-2020-65-12-757-766>.
- [2] P.S. Wikramaratna, R.S. Paton, M. Ghafari, J. Lourenço, Estimating the false-negative test probability of SARS-CoV-2 by RT-PCR, *Euro Surveill.* 25 (2020). <https://doi.org/10.2807/1560-7917.ES.2020.25.50.2000568>.
- [3] O. Sharma, A.A. Sultan, H. Ding, C.R. Triggler, A review of the progress and challenges of developing a vaccine for COVID-19, *Front. Immunol.* 11 (2020) 585354. <https://doi.org/10.3389/fimmu.2020.585354>.
- [4] A. Wajsborg, et al., Robust neutralizing antibodies to SARS-CoV-2 spike receptor-binding domain bound to the ACE2 receptor, *Science* 370 (2020) 1227–1230. <https://doi.org/10.1126/science.abd7728>.
- [5] J. Lan, et al., Structure of the SARS-CoV-2 spike receptor-binding domain bound to the ACE2 receptor, *Nature* 581 (2020) 215–220. <http://doi.org/10.1038/s41586-020-2180-5>.
- [6] G.A. Poland, Tortoises, hares, and vaccines: a cautionary note for SARS-CoV-2 vaccine development, *Vaccine* 38 (2020) 4219–4220. <https://doi.org/10.1016/j.vaccine.2020.04.073>.
- [7] A. Griffoni, et al., A sequence homology and bioinformatic approach can predict candidate targets for immune responses to SARS-CoV-2, *Cell Host Microbe* 27 (2020) 671–680, e2. <https://doi.org/10.1016/j.chom.2020.03.002>.
- [8] M. Tré-Hardy, et al., Analytical and clinical validation of an ELISA for specific SARS-CoV-2 IgG, IgA, and IgM antibodies, *J. Med. Virol.* 15 (2020). <https://doi.org/10.1002/jmv.26303>. <https://doi.org/10.1002/jmv.26303>.
- [9] N. Ravi, D.L. Cortade, E. Ng, S.X. Wang, Diagnostics for SARS-CoV-2 detection: a comprehensive review of the FDA-EUA COVID-19 testing landscape, *Biosens. Bioelectron.* 165 (2020) 112454. <https://doi.org/10.1016/j.bios.2020.112454>.
- [10] C. Wang, et al., Sensitive and simultaneous detection of SARS-CoV-2-specific IgM/IgG using lateral flow immunoassay based on dual-mode quantum dot

- nanobeads, *Anal. Chem.* 92 (2020) 15542–15549. <https://doi.org/10.1021/acs.analchem.0c03484>.
- [11] L. Anfossi, F. Di Nardo, S. Cavalera, C. Giovannoli, C. Baggiani, Multiplex lateral flow immunoassay: an overview of strategies towards high-throughput point-of-need testing, *Biosensors* 9 (2018) 2. <https://doi.org/10.3390/bios9010002>.
- [12] O. Miocević, et al., Quantitative lateral flow assays for salivary biomarker assessment: a review, *Front. Public Health* 5 (2020) 133. <https://doi.org/10.3389/fpubh.2017.00133>.
- [13] Y.M. Liu, et al., A carbohydrate-binding protein from the edible lablab beans effectively blocks the infections of influenza viruses and SARS-CoV-2, *Cell Rep.* 32 (2020c), 108016. <http://doi.org/10.1016/j.celrep.2020.108016>.
- [14] L.A. Silva, H. Sanchez San Blas, D. Peral García, A. Sales Mendes, G. Villarubia González, An architectural multi-agent System for a pavement monitoring System with pothole recognition in UAV images, *Sensors* 20 (2020) 6205. <https://doi.org/10.3390/s20216205>.
- [15] A. Bochkovskiy, C.Y. Wang, H.Y.M. Liao, in: *Yolov4: Optimal Speed and Accuracy of Object Detection*, 2020, p. 10934, arXiv. preprint arXiv. 2004.
- [16] W. Fang, L. Wang, P. Ren, Tinier-YOLO, A real-time object detection method for constrained environments, *IEEE Access* 8 (2020) 1935–1944. <https://doi.org/10.1109/ACCESS.2019.2961959>.
- [17] G. Liu, J.C. Nouaze, P.L. Touko Mbouembe, J.H. Kim, YOLO-tomato: a robust algorithm for tomato detection based on YOLOv3, *Sensors* 20 (2020a) 2145. <https://doi.org/10.3390/s20072145>.
- [18] P.F. Liu, Y. Wang, Y.T. Liu, C.M. Huang, Vaccination with killed but metabolically active *E. coli* over-expressing hemagglutinin elicits neutralizing antibodies to H1N1 swine origin influenza A virus, *J. Nat. Sci.* 3 (2017) e317.
- [19] M.K. Gautier, S.D. Ginsberg, A method for quantification of vesicular compartments within cells using 3D reconstructed confocal z-stacks: comparison of ImageJ and Imapris to count early endosomes within basal forebrain cholinergic neurons, *J. Neurosci. Methods* 350 (2020) 109038. <https://doi.org/10.1016/j.jneumeth.2020.109038>.
- [20] A. Srivastava, J.P. Hanig, Quantitative neurotoxicology: potential role of artificial intelligence/deep learning approach, *J. Appl. Toxicol.* 2 (2020). <https://doi.org/10.1002/jat.4098>.
- [21] S. Jakhmola, et al., Recent updates on COVID-19: a holistic review, *Heliyon* 6 (2020), e05706. <https://doi.org/10.1016/j.heliyon.2020.e05706>.
- [22] M. Bianchi, D. Benvenuto, M. Giovanetti, et al., Sars-CoV-2 envelope and membrane proteins: structural differences linked to virus characteristics? *BioMed Res. Int.* 2020 (2020) 4389089.
- [23] N. Khairkhan, M.R. Aghasadeghi, A. Namvar, A. Bolhassani, Design of novel multi-epitope constructs-based peptide vaccine against the structural S, N and M proteins of human COVID-19 using immunoinformatics analysis, *PLoS One* 15 (2020), e0240577. <https://doi.org/10.1371/journal.pone.0240577>.
- [24] M.D. Keller, et al., SARS-CoV-2 specific T cells are rapidly expanded for therapeutic use and target conserved regions of the membrane protein, *Blood* 136 (2020) 2905–2917. <https://doi.org/10.1182/blood.2020008488>.
- [25] Y. Zheng, et al., Severe acute respiratory syndrome coronavirus 2 (SARS-CoV-2) membrane (M) protein inhibits type I and III interferon production by targeting RIG-I/MDA-5 signaling, *Signal Transduct. Target Ther.* 5 (2020) 299. <https://doi.org/10.1038/s41392-020-00438-7>.
- [26] A. Park, A. Iwasaki, Type I and type III interferons - induction, signaling, evasion, and application to combat COVID-19, *Cell Host Microbe* 27 (2020) 870–878. <https://doi.org/10.1016/j.chom.2020.05.008>.
- [27] C.O. Barnes, et al., SARS-CoV-2 neutralizing antibody structures inform therapeutic strategies, *Nature* 588 (2020) 682–687. <https://doi.org/10.1038/s41586-020-2852-1>.
- [28] C. Cassidy, et al., FDA efficiency for approval process of COVID-19 therapeutics, *Infect. Agents Canc.* 15 (2020) 73. <https://doi.org/10.1186/s13027-020-00338-z>.
- [29] M. Michel, et al., Evaluating ELISA, immunofluorescence, and lateral flow assay for SARS-CoV-2 serologic assays, *Front. Microbiol.* 11 (2020) 597529. <https://doi.org/10.3389/fmicb.2020.597529>.
- [30] A.L. Nelson, J.M. Reichert, Development trends for therapeutic antibody fragments, *Nat. Biotechnol.* 27 (2009) 331–337. <http://doi.org/10.1038/nbt0409-331>.
- [31] E. O Murchu, et al., Immune response following infection with SARS-CoV-2 and other coronaviruses: a rapid review, *Rev. Med. Virol.* 23 (2020), e2162. <https://doi.org/10.1002/rmv.2162>.
- [32] L. Björck, L. Protein, A novel bacterial cell wall protein with affinity for Ig L chains, *J. Immunol.* 140 (1988) 1194–1197.